IEEE Access
Multidisciplinary | Rapid Review | Open Access Journal

Received July 14, 2019, accepted July 24, 2019, date of publication August 2, 2019, date of current version August 15, 2019.

Digital Object Identifier 10.1109/ACCESS.2019.2932940

Performance Criterion of Phasor Measurement Units for Distribution System State Estimation

JONGHOEK KIM[1], (Member, IEEE), HYUN-TAE KIM[2], AND SUNGYUN CHOI[2], (Member, IEEE)
[1]Electrical and Electronic Convergence Department, Hongik University, Sejong 30016, South Korea
[2]School of Electrical Engineering, Korea University, Seoul 02841, South Korea

Corresponding author: Sungyun Choi (sungyun.choi@ieee.org)

This work was supported in part by the Korea University Grant, and in part by the Human Resources Program in Energy Technology of the Korea Institute of Energy Technology Evaluation and Planning (KETEP) granted financial resource from the Ministry of Trade, Industry and Energy, South Korea, under Grant 20174030201820.

ABSTRACT A phasor measurement unit (PMU) is a device that can directly measure the phase angles of voltages and currents, with high accuracy, using accurate time signals. Hence, PMUs have originally been used to improve the accuracy of transmission system state estimation. The merit of PMUs, further, extends the scope of its application to distribution system state estimation (DSSE), which has recently been studied because of the growing needs for distribution system management due to high levels of distributed energy resources. More importantly, the scarcity of measuring sensors in distribution systems highlights the role of PMUs for the DSSE. However, the full deployment of PMUs in distribution systems is practically impossible because of the high installation costs and geographically large size of these systems. Therefore, this paper investigates the adequate and economic performance of PMUs to meet the DSSE requirement with respect to the estimation accuracy. The accuracy of different PMU performance classes and the accuracy of various measurement types are first defined. Different sets of measurements are then assigned to different meter locations in a testbed that is a three-phase unbalanced, asymmetric system. Various performance metrics for each case study are computed and compared from the numerical simulation results.

INDEX TERMS Distribution system state estimation, phasor measurement unit, power system state estimation.

I. INTRODUCTION

In the electric power industry, the time synchronism of measurement data is one of the most critical requirements for wide area monitoring systems since it enables the determination of the phase angles of all buses. Traditionally, transmission system operators have utilized state estimation (SE) to compute these phase angles by collecting all measurements from supervisory control and data acquisition (SCADA) systems; however, the collection of a set of measurements for a specific time takes 2 s or longer, which leads to a low accuracy of the SE results.

In coping with this issue, phasor measurement units (PMUs) capable of directly and accurately measuring phasor angles based on the global positioning system (GPS) have been used to improve the SE performance in terms of the estimation accuracy and computational speed [1], [2]. In addition to the improvement of the SE performance, the direct measurement of phase angles enables fast phasor sampling (i.e., maximum of 120 samples per second), providing numerous benefits such as dynamic SE [3], measurement-based operation [4], and distributed SE [5].

The importance of distribution system state estimation (DSSE) has recently grown because of the increasing penetration of distributed generations (DGs) and power-electronics-based devices [6]–[10], as well as because of the need for voltage regulations [11], [12]. Additionally, [13] presented a multiarea state estimation approach to address numerous nodes and different voltage levels. The approach was based on two steps, with the first step being the use of local state estimators and the second step being the integration of measurement information from adjacent zones and performance of the linear state estimation. The DSSE can also be applied to AC-DC hybrid distribution systems using a three-stage distributed state estimation with the SCADA and PMU measurements [14].

The PMU can play an essential role in the DSSE when considering the lack of sensors in distribution systems. The time

The associate editor coordinating the review of this manuscript and approving it for publication was Guido Carpinelli.

synchronism and the high sampling rate enhance the DSSE performance in terms of the estimation accuracy and computation time [15] and further evolve the grid analytics by pairing with big data [16]. Meanwhile, [17] proposed a state estimation based on the ensemble Kalman filter to enhance the current estimation accuracy. The method utilized a pseudo-measurement based on historical data and the PMU measurement and detached the power flow equations from the estimator. In [18], the authors analyzed factors for the accurate estimation of voltage profiles from the DSSE by mathematically showing how the estimation uncertainty depends on the PMU or hybrid measurement systems.

However, given full employment of PMUs, the major challenges that lie in the PMU applications for the DSSE include high installation costs caused by the size of the distributed networks. A robust method for the placement of PMUs and voltage magnitude meters based on the submodular saturation algorithm was presented to cope with the worst case of estimation at peak loads [19]. However, the method only considered a single accuracy for the PMU; hence, selecting an economic time-synchronism protocol and the corresponding PMUs that can provide adequate performance ensuring grid observability and obtaining sufficiently accurate, real-time network models is highly important. For this purpose, this study investigates the optimum level of accuracy of PMU measurements for the DSSE to be able to provide the real-time operating conditions of distribution systems with a high accuracy.

This paper first defines the different levels of the PMU accuracy based on time synchronism and then formulates the measurement model for the DSSE based on the measurement type. The impact of the PMU accuracy on the DSSE performance is then evaluated by testing different measurement sets (including PMUs with different accuracies, SCADA measurements, and smart meters) at the various locations of the distribution system. The performance criteria are studied based on the experimental test results and compared with each other in terms of the accuracy and the robustness against realistic field conditions, which eventually enlarges a vision of how to select adequate PMU accuracy.

The remainder of this paper is structured as follows. Firstly, Section II investigates the requirements of the PMU accuracy for the DSSE, and then Section III explains the mathematical formulation of the DSSE. In Section IV, the test distribution systems for the numerical simulations are described, followed by observations on the case-study results. Finally, this paper is concluded in Section V.

II. PMU ACCURACY REQUIREMENTS FOR THE DSSE

Many factors affect the accuracy of PMU measurements, for example, installation of hardware equipment, distribution methods of time signals, time-synchronism protocols, phasor estimation algorithms, and filter designs. A dedicated GPS receiver can provide a PMU with highly precise time signals, but installing the GPS receiver for each individual PMU may be impossible because of high installation costs and spatial constraints. Therefore, time signals can be distributed to multiple PMUs through twisted pair wires or coaxial cables in accordance with the inter-range instrumentation group B time codes [20]. Alternatively, time information can also be transferred via computer networks according to the network time protocol [21] or the precision time protocol [22], [23]. The time accuracy can be the order of microseconds or a few milliseconds depending on communication lines or time-synchronism protocols with different precisions and latencies. Even though a PMU acquires accurate time information, phasor estimation algorithms or pre-processing (or post-processing) filters definitely affect the accuracy of finally-estimated phasor values. Moreover, these algorithms or filters are quite vendor-specific.

Considering these various factors determining the PMU accuracy, defining the PMU requirements for the DSSE with the aforementioned factors is a time-consuming task; hence, the request for keeping phasor values extracted by a PMU within the required limits for the DSSE is more viable. As an example, [24] and [25] defined a metric called the total vector error (TVE) to test the PMU performance in various environments. The TVE can be calculated as follows:

$$TVE \equiv \frac{\left|\vec{V}_{measured} - \vec{V}_{true}\right|}{\left|\vec{V}_{true}\right|}, \tag{1}$$

where $\vec{V}_{measured}$ is the phasor measured by a PMU, and $\vec{V}_{true}$ is the true phasor.

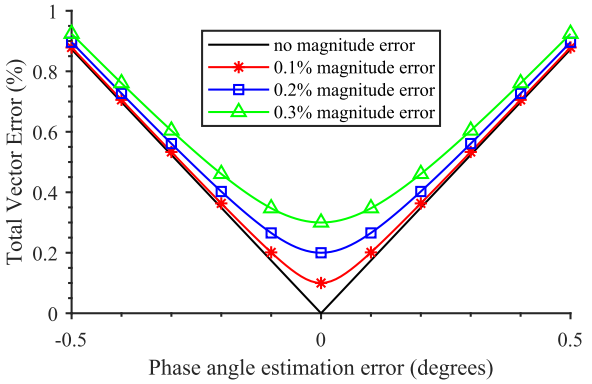

FIGURE 1. TVE for different magnitude errors (i.e., 0%, 0.1%, 0.2%, and 0.3%) and angle errors (from −0.5 to 0.5°) [25].

Notice that the TVE simultaneously reflects the magnitude errors and angle ones of phasors. As described in Fig. 1, the TVE of a phasor is larger than the magnitude error of the phasor unless the phase error is zero. The TVE increases almost up to 1%, even with a magnitude error of 0.1%, when a phase angle is deviated from its true value by 0.5°, indicating that the phase angle error has a considerable effect on the TVE in most cases. Hence, the TVE is a practical metric for the PMU performance.

This TVE metric was used to verify whether or not a proposed phasor estimation algorithm or filter [26]–[28]

meets the desired level of the PMU performance compliant with [24] and [25]. Accordingly, [26] and [27] assured that the proposed filters improved the PMU performance to meet a basic requirement of the TVE (i.e., 1%), and [28] proposed an adaptive algorithm of phasor estimation based on a Taylor-Fourier transform, which extracted phasors within the TVE limits.

In an attempt to assess the DSSE performance, this paper utilizes the TVE metric in a way that investigates whether or not the TVEs of all the estimated voltage phasors are within the allowable range. In [24], a TVE of 1% is defined as the allowed maximum steady-state error. Note that 1% TVE corresponds to a phase error of 0.01 radians (i.e., 0.57°) and a time error of ± 26 μs for a 60Hz system. The requirement of the 1% TVE is a common standard at the transmission level, but this study proposes a methodology of finding the adequate accuracy of PMUs to meet the desired criterion in the distribution system; hence, one must note that the 1% TVE is not a strict criterion; rather, the criterion can be selected in accordance with an operational requirement or a DSSE application.

It is, however, necessary to point out that the TVE should be lower than 1% at the boundary between the distribution and transmission system because of the operational needs for coordination between them. For example, accurate phasor information can be used to reconnect an islanded microgrid and the transmission side, which requires the resynchronization [29]. In addition, the accurate estimation of the phase angles is of prime importance for the computation of the active power loss in distribution lines, real-time detection of the reverse power flow of DGs [29], system reconfiguration [30], and resynchronization and reconnection of the DG to the grid.

The ultimate objective of this paper is to find the time-synchronism accuracy of PMUs, which will be installed in distribution systems, such that the DSSE performance criterion is satisfied. As mentioned earlier, the performance of the PMUs considerably relies on various factors, including time-synchronism protocols and manufacturers; thus, referring to the PMU performance classes defined in [31] on the basis of the time-synchronism accuracy will be more practical than defining the requirements for each individual factor. Table 1 lists the PMU performance classes in [31].

TABLE 1. Accuracy requirements defined in IEC 61850-5 [31].

Performance class	Max deviation in 60Hz	
T5	1 μs	$(= 0.0216°)$
T4	4 μs	$(= 0.0864°)$
T3	25 μs	$(= 0.54°)$
T2	100 μs	$(= 2.16°)$
T1	1 ms	$(= 21.6°)$
T0	10 ms	$(= 216°)$

Even though a PMU can provide the time measurement accuracy on the order of microseconds, the measurement errors are inevitably introduced from the instrumentation channel including instrument transformers (e.g., potential or current transformers), burden resistances, attenuators, and cables [32]. This error, which is a systematic bias, corresponds to a phase error of up to ± 277.8 μs, that is, $\pm 6°$ in a 60 Hz system. Several efforts have been made to address the error [33], [34]. Meliopoulos *et al.* proposed an empirical approach to correct the errors induced from the instrumentation channel by generating a single transfer function containing all models along the channel from the high voltage side to the measurement output [33]. A hybrid, distributed state estimation that utilizes measurements from both the SCADA system and the local PMU was presented in [34]. The method considered the phase error caused by an unknown delay and exchanged limited information between adjacent areas, thereby reducing the communication burdens.

Although any systematic and unknown errors such as the instrument channel error might be introduced to the PMU measurements, the error can be dealt with using many calibrating methods. Moreover, the investigation on the impact of the error on the PMU accuracy and, subsequently, the DSSE performance is out of the scope of this paper. We instead assume that the performance class in Table 1 refers to the accuracy of the output measurement with respect to the true value. That is to say, the accuracy reflects all the errors generated from the high-voltage side to the output.

The cable distance between a GPS receiver and a PMU is one of the significant sources of time signal errors because a long cable distance causes the latency of the GPS signal delivery. However, as in the case of the instrumentation channel error, the errors induced from the communication latency of the GPS signals are reflected in the performance class.

III. DSSE FORMULATION

A. WLS STATE ESTIMATION

The SE algorithm used in this study is the well-known weighted least-squares (WLS) method, which is a suitable solver for the DSSE because the method has a consistent and good-quality performance when applied on distributed networks [35]. The measurement model can mathematically be defined as follows:

$$z = h(x) + \eta, \tag{2}$$

where $z \in \mathbb{R}^m$ is the measurement vector; m is the number of measurements; $x \in \mathbb{R}^n$ is the state vector; n is the number of states; $h : \mathbb{R}^n \to \mathbb{R}^m$ is the vector of functions relating states to measurements; $\eta \backsim \mathcal{N}(0, R)$ is the zero-mean Gaussian noise vector with the error covariance matrix $R(= \text{ diag}\left\{\sigma^2(z_1), \sigma^2(z_2), \ldots, \sigma^2(z_m)\right\})$; and $\sigma(z_i)$ is the standard deviation of the i-th measurement.

The WLS problem can be formulated to minimize the following objective function:

$$\min J(x) = \eta^T W \eta = [h(x) - z]^T W [h(x) - z], \tag{3}$$

where $W(= R^{-1})$ is the weight matrix. In the end, the states can be estimated as follows using the Newton-Raphson

iterative method:

$$x^{i+1} = x^i - (H^T WH)^{-1} H^T W \left(h(x^i) - z \right), \tag{4}$$

where i is the iteration index, and H is the Jacobian matrix of $h(x)$.

B. DISTRIBUTION LINE MODEL

The major difference of the DSSE from the transmission system SE is that the distribution systems have asymmetric line structures and operate in unbalanced conditions. In this sense, the distribution lines must be modeled in three phases, considering mutual inductances and capacitances. Fig. 2 illustrates the three-phase π-model of the distribution lines connecting two adjacent buses, which is used to formulate the measurement models in the proposed approach.

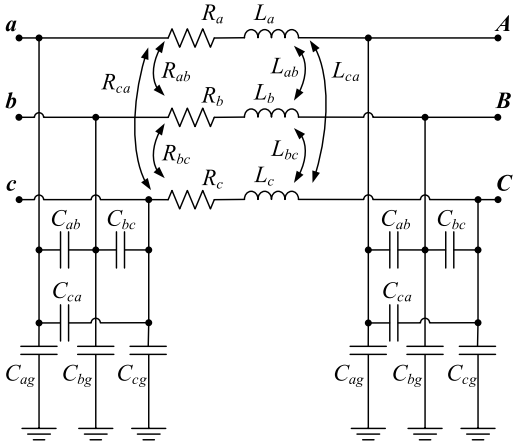

FIGURE 2. Six-port π-model of the distribution lines.

TABLE 2. Measurement descriptions.

Measurement type	Measuring unit	Measured quantities
Branch	SCADA	$\lvert\widetilde{V}\rvert$, P, Q
Branch	PMU	$\widetilde{V}$, $\widetilde{I}$
Injection	Smart Meter	$\lvert\widetilde{V}\rvert$, P, Q
Injection	PMU	$\widetilde{V}$, $\widetilde{I}$
Virtual	(N/A)	Physical Laws

($\widetilde{V}$ and $\widetilde{I}$ are the voltage and the current phasor, respectively.)

C. MEASUREMENT TYPE

Table 2 shows the following three types of measurements considered for the DSSE: branch, injection, and virtual measurements. The tilde superscript notation represents the phasor value. First, the branch measurements are typically located in the distribution lines to monitor the voltage, current, and real/reactive power. SCADA systems have previously obtained the voltage magnitude ($|\widetilde{V}|$) and the real/reactive power (P, Q). Now, PMUs, including transmission-level PMUs and μPMUs [4], [16], [29], [36], [37], can replace the measurements by directly measuring voltage and current phasors ($\widetilde{V}$ and $\widetilde{I}$).

Smart meters or PMUs can be employed as the injection measurements. Smart meters measure the voltage magnitude and real/reactive power like SCADA systems, but its accuracy is generally lower than that in SCADA systems because the functional capabilities of smart meters may be limited when it comes to many radial (or meshed) distribution feeders and, as a result, the consideration of their economic installation costs. The loads and generators in the general SE are modeled as equivalent power injections with real/reactive power [38]; therefore, the same rules apply on DGs and loads for the DSSE.

Lastly, virtual measurements are introduced based on physical laws such as Kirchhoff's current law (KCL). For example, a virtual measurement based on KCL is applicable to any buses without power injections.

D. MEASUREMENT MODEL FORMULATION

Given $\mathcal{N}_b$ buses, n state variables corresponding to the voltage phasors (i.e., $\widetilde{V}_1, \widetilde{V}_2, \ldots, \widetilde{V}_{\mathcal{N}_b}$) are defined as $x_1, x_2, \ldots, x_n$, where $n = 2\mathcal{N}_b$. Note that a pair of state variables refers to the real and imaginary numbers of the corresponding voltage phasor.

Before formulating the measurement models, the equations of the branch current and real/reactive power must first be defined based on the distribution line model in Fig. 2. When the device model of a distribution line j is expressed as follows:

$$[\widetilde{I}_a, \widetilde{I}_b, \widetilde{I}_c, \widetilde{I}_A, \widetilde{I}_B, \widetilde{I}_C]^T = Y[\widetilde{V}_a, \widetilde{V}_b, \widetilde{V}_c, \widetilde{V}_A, \widetilde{V}_B, \widetilde{V}_C]^T, \tag{5}$$

where Y is the admittance matrix; $\widetilde{I}_a, \widetilde{I}_b, \widetilde{I}_c, \widetilde{I}_A, \widetilde{I}_B$, and $\widetilde{I}_C$ are the current phasor at nodes a, b, c, A, B, and C, respectively; and $\widetilde{V}_a$, $\widetilde{V}_b$, $\widetilde{V}_c$, $\widetilde{V}_A$, $\widetilde{V}_B$, and $\widetilde{V}_C$ are the voltage phasors at nodes a, b, c, A, B, and C, respectively. A current phasor at node k toward line j is denoted by $\widetilde{I}_j (= I_{j,r} + jI_{j,i})$, which is expressed as (6).

$$I_{j,r} = \sum_{a=1}^{n} y_a x_a, \quad I_{j,i} = \sum_{b=1}^{n} y_b x_b, \tag{6}$$

where y_a and y_b are the coefficients determined by (5).

Denoting a phasor voltage at node k by $\widetilde{V}_k (= x_r + jx_i)$, the real and reactive power at bus k toward line j (i.e., P_j and Q_j) can be obtained by (7) and (8), respectively.

$$P_j = x_r I_{j,r} + x_i I_{j,i} = \sum_{a=1}^{n} y_a x_r x_a + \sum_{b=1}^{n} y_b x_i x_b, \tag{7}$$

$$Q_j = x_i I_{j,r} - x_r I_{j,i} = \sum_{a=1}^{n} y_a x_i x_a - \sum_{b=1}^{n} y_b x_r x_b. \tag{8}$$

One can now formulate a measurement model for the DSSE according to its measurement type and quantity as described in the sub-sections that follow.

1) VOLTAGE MAGNITUDE SQUARED (BRANCH & INJECTION)

$\widetilde{V}_k$ is expressed in Cartesian coordinates with x_r and x_i; hence, $|\widetilde{V}_k|^2$ is used as a measurement such that the square root is not involved in its measurement model. The measurement model of $|\widetilde{V}_k|^2$ is expressed as follows:

$$z_{|\widetilde{V}_k|^2} = x_r^2 + x_i^2 + \eta, \tag{9}$$

where x_r and x_i are the states referring to the real and imaginary parts of $\widetilde{V}_k$, respectively. The standard deviation of $z_{|\widetilde{V}_k|^2}$ can be computed as follows based on the classical uncertainty propagation theory [39]:

$$\sigma(z_{|\widetilde{V}_k|^2}) = 2|\widetilde{V}_k|\sigma(|\widetilde{V}_k|). \tag{10}$$

2) REAL/REACTIVE POWER (BRANCH)

The measurement models for P_j and Q_j are formulated as follows based on (7) and (8), respectively:

$$z_{P_j} = P_j + \eta, \quad z_{Q_j} = Q_j + \eta. \tag{11}$$

3) REAL/REACTIVE POWER (INJECTION)

Measurement models for real/reactive power injection measurements (i.e., $z_{P_{inj}}$ and $z_{Q_{inj}}$) obtained by smart meters can be created based on KCL, yielding the following equations:

$$z_{P_{inj}} = -\sum_{j=1}^{l} P_j + \eta, \quad z_{Q_{inj}} = -\sum_{j=1}^{l} Q_j + \eta, \tag{12}$$

where l is the number of adjacent lines at bus k. The direction of the injections is toward the injections themselves.

4) VOLTAGE PHASOR

A PMU is capable of directly measuring $\widetilde{V}_k$, formulating the following measurement models:

$$z_{V_r} = x_r + \eta, \quad z_{V_i} = x_i + \eta, \tag{13}$$

where V_r and V_i are the real and imaginary values of $\widetilde{V}_k$, respectively, and their measurements can be calculated by the voltage magnitude ($|\widetilde{V}_k|$) and the phase angle (θ_{V_k}) that are normally provided by a PMU. In other words, $V_r = |\widetilde{V}_k|\cos(\theta_{V_k})$ and $V_i = |\widetilde{V}_k|\sin(\theta_{V_k})$. Hence, the standard deviation of z_{V_r} and z_{V_i} can be computed as follows:

$$\sigma(z_{V_r}) = \sqrt{\left(\frac{\partial z_{V_r}}{\partial|\widetilde{V}_k|}\right)^2 \sigma^2(|\widetilde{V}_k|) + \left(\frac{\partial z_{V_r}}{\partial\theta_{V_k}}\right)^2 \sigma^2(\theta_{V_k})}, \tag{14}$$

$$\sigma(z_{V_i}) = \sqrt{\left(\frac{\partial z_{V_i}}{\partial|\widetilde{V}_k|}\right)^2 \sigma^2(|\widetilde{V}_k|) + \left(\frac{\partial z_{V_i}}{\partial\theta_{V_k}}\right)^2 \sigma^2(\theta_{V_k})}. \tag{15}$$

5) CURRENT PHASOR (BRANCH)

The measurement models for $\widetilde{I}_j$ are created as follows based on (6):

$$z_{I_{j,r}} = I_{j,r} + \eta, \quad z_{I_{j,i}} = I_{j,i} + \eta. \tag{16}$$

6) CURRENT PHASOR (INJECTION)

When a phasor of a current injection is denoted by $\widetilde{I}_{inj}(= I_{inj,r} + jI_{inj,i})$, its measurement model can be formulated based on KCL as (17), consisting of adjacent branch currents (i.e., $\widetilde{I}_j$).

$$z_{I_{inj,r}} = -\sum_{j=1}^{l} I_{j,r} + \eta, \quad z_{I_{inj,i}} = -\sum_{j=1}^{l} I_{j,i} + \eta. \tag{17}$$

Notice that the direction of the current injections is toward the injections themselves. As is the case of the voltage phasor measurements, the current phasor measurements, including $z_{I_{j,r}}$, $z_{I_{j,i}}$, $z_{I_{inj,r}}$, and $z_{I_{inj,i}}$, are computed by the current magnitude and phase angle that the PMUs provide. Their standard deviations can be obtained based on the uncertainty propagation theory.

7) VIRTUAL MEASUREMENT (KCL)

The measurement models for the KCL virtual measurements are formulated as follows:

$$z_{I_{\mathrm{KCL},r}} = \sum_{j=1}^{l} I_{j,r} + \eta, \quad z_{I_{\mathrm{KCL},i}} = \sum_{j=1}^{l} I_{j,i} + \eta, \tag{18}$$

where $z_{I_{\mathrm{KCL},r}} = 0$ and $z_{I_{\mathrm{KCL},i}} = 0$ by the KCL definition. In general, the standard deviation of the virtual measurements are manually selected with high accuracy.

E. CONSIDERATION OF THE MODEL UNCERTAINTY

The system model accuracy is critical in the DSSE performance. This study depends on the assumption that the accurate system model (i.e., network impedances) is provided, and thus, the uncertainty in the model might significantly affect the accuracy of the DSSE results. In this sense, the network model integrity must be continuously checked along with the DSSE. The parameter estimation and the topology processor play an essential role in obtaining accurate information on the system model [6]. The network impedance is reflected in the computation of current and active/reactive power as expressed in (6) to (8), which are used for the formulation of measurement models of real/reactive power branches/injections, current branches/injections, and virtual measurements. The study on the effect of uncertainty in the network model is out of the scope of this paper but left in further research.

IV. CASE STUDY

A 15-bus test system with three-phase asymmetric structures and unbalanced operations is used to investigate the effect of the PMU accuracy on the DSSE performance. This test system is similar to those tested in [15] and [40]. Fig. 3 depicts this test system, with the marking meter locations having red/blue and circles/stars/triangles/squares.

A. TEST CONDITIONS

The distribution line parameters per mile used in this study (Fig. 2) are nearly identical to those of configuration 300 in

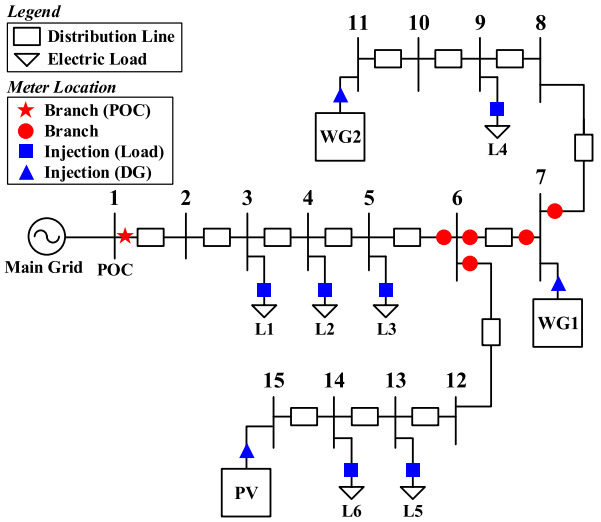

FIGURE 3. Distribution system under testing. For clarification, POC, L, PV, and WG denote the point of connection, load, photovoltaic, and wind generator, respectively.

TABLE 3. Distribution line parameters per mile.

Resistance	Value (Ω)	Reactance	Value (Ω)	Susceptance	Value (μS)
R_a	1.3368	$\omega_0 L_a$	1.3343	$2\omega_0 C_{ag}$	5.3350
R_b	1.3238	$\omega_0 L_b$	1.3569	$2\omega_0 C_{bg}$	5.0979
R_c	1.3294	$\omega_0 L_c$	1.3471	$2\omega_0 C_{cg}$	4.8880
R_{ab}	0.2102	$\omega_0 L_{ab}$	0.5779	$2\omega_0 C_{ab}$	–1.5313
R_{bc}	0.2066	$\omega_0 L_{bc}$	0.4591	$2\omega_0 C_{bc}$	–0.9943
R_{ca}	0.2130	$\omega_0 L_{ca}$	0.5015	$2\omega_0 C_{ca}$	–0.6212

($\omega_0 = 2\pi f$)

TABLE 4. Distribution line length (mile).

Section	Length	Section	Length	Section	Length
B1 to B2	0.4886	B6 to B7	5.6301	B6 to B12	0.00189
B2 to B3	0.0819	B7 to B8	0.00189	B12 to B13	1.4342
B3 to B4	0.2457	B8 to B9	0.05871	B13 to B14	0.3466
B4 to B5	6.1042	B9 to B10	0.4834	B14 to B15	0.8456
B5 to B6	7.1023	B10 to B11	1.4503		

(B denotes Bus.)

the IEEE 34 node test feeder [41] (Table 3). Table 4 also shows the line length of each section. Table 5 lists the power injection parameters, including the electric loads and the DGs. The positive direction of the real/reactive power is toward the corresponding injection unit.

The nominal parameters of the test system are 24.9 kV, 400 kVA, and 60 Hz, which are applied on the branch measurements. The maximum three-phase rating of the power injections is approximately 108 kVA according to the given load and generation conditions in Table 5; therefore, a rating of 150 kVA is given to the injection measurements.

TABLE 5. Power injection parameters.

Bus #	Type	P (kW)			Q ($kVar$)		
		Ph-A	Ph-B	Ph-C	Ph-A	Ph-B	Ph-C
3	L	33.4	40	33.4	4.1	5	3.8
4	L	20	20	16.6	2.3	3	1.9
5	L	0	40.9	9	0	4	0
9	L	0	0	49.1	0	0	5.5
13	L	40	30	19.8	4.8	3.1	2.2
14	L	28	20	16.6	3.4	2.6	1.9
7	DG	-24	-25	-23	-3.5	-3.6	-3.3
11	DG	-12	-11	-9	-1.8	-1.6	-1.3
15	DG	-31	-29	-30	-4.5	-4.2	-4.3

Four meter locations are used (Fig. 3), and test cases (Table 6) are designed in such a way that each location has a different type of a measuring unit (e.g., SCADA systems, smart meters, and PMUs) with different accuracies. Different performance classes defined in Table 1 are selected in the case of the PMUs. Note that the virtual measurements based on KCL are applied to buses 2, 8, 10, and 12 for all cases.

However, the branch measurements at the point of connection (POC) are highly crucial because at least a reference measurement is needed in order for the distribution management systems (DMSs) to autonomously operate the distributed networks and because the transmission system operators monitor voltages and currents at the point nearest to the transmission side. The re-synchronization of an islanded microgrid to the main grid, followed by the seamless reconnection between them, also highly relies on the accurate measurement of the phase angle at the POC. In this manner, a T5-class PMU is assumed to be always installed at the POC, providing highly accurate, time-synchronized branch measurements.

As specified in [25], the desired accuracy of the voltage and the current magnitude measured by the PMU is 0.1%, which is, thus, given to the standard deviations of $|\widetilde{V}_k|$, $|\widetilde{I}_j|$, and $|\widetilde{I}_{inj}|$. Regarding the phase angle measurement that the PMU provides, its standard deviation can be obtained by dividing its maximum deviation (Table 1) by $\sqrt{3}$ [39].

The typical standard deviations for the SCADA measurements are given to the voltage magnitude and power flows of 1% and 2%, respectively [1]. The standard deviations for the remainder are 0.1% for the virtual measurements, 1% for the voltage magnitude from the smart meters, and 3% for the power injections from the smart meters. The SCADA measurement and the smart meter have a non-GPS time tagging, thereby introducing larger measurement errors than the PMU measurement. Hence, the standard deviations of the measurement errors of the SCADA and the smart meter reflect less accurate time synchronization. More specifically, the standard deviations of the SCADA measurement and the smart meter vary by practical conditions such as communication network latency, time-tagging protocols, and filters.

In reality, the zero-mean Gaussian noises are added to all the measurements with the corresponding standard deviations. Furthermore, 300 samples with different measurement noises are tested for each test case and evaluated based on the performance metrics. As long as the DSSE uses the SCADA and smart meters, the time interval of the state estimation is in the order of minutes.

B. PERFORMANCE METRICS

Several metrics are computed to evaluate the DSSE performance after estimating the present states using the DSSE.

1) CONFIDENCE LEVEL

The confidence level, which can be quantified by the well-known chi-square test, indicates the probability of the goodness of fit of measurements to a system model (i.e., how well the measurements are consistent with the model). The confidence level is computed as follows with the degree of freedom, ν, and the chi-square critical value, ζ:

$$\Pr\left[\chi^2 \geq \zeta\right] = 1.0 - \Pr\left[\chi^2 \leq \zeta\right] = 1.0 - \Pr(\zeta, \nu), \quad (19)$$

such that

$$\nu = m - n, \quad \zeta = \sum_{i=1}^{m} \left(\frac{h_i(\hat{x}) - z_i}{\sigma(z_i)}\right)^2,$$

where χ^2 denotes the chi-square random variables; $\Pr(\zeta, \nu)$ is the cumulative distribution function of χ^2 with ν; and $\hat{x}$ is the best estimate of the states.

If the confidence level maintains at 100% during the operation, the real-time measurements are consistent with the system model, thereby indicating that no bad data exist as long as the model is accurate. On the other hand, the low confidence level implies the existence of any bad data, which must be followed by the bad data detection process.

2) TVE

Considering the necessary conditions of the PMUs (i.e., the TVE of the phasors measured by the PMUs should be within 1%) specified in [25], applying a TVE requirement on the voltage phasors estimated by the DSSE could be a reasonable criterion of the DSSE performance evaluation.

3) ROOT MEAN SQUARE ERROR (RMSE)

The RMSE between the estimated states and their true values over all the samples indicates how close the estimation is to its true value. The RMSE of a specific state x is calculated as follows:

$$\text{RMSE}_x = \sqrt{\sum_{i=1}^{\mathcal{N}_s} (x_i - \hat{x}_i)^2}, \quad (20)$$

where $\mathcal{N}_s$ is the total number of samples (i.e., 300).

4) ABSOLUTE ERROR OF THE TOTAL LINE-LOSS ESTIMATION ($|\mathcal{E}_{P_{loss}}|$)

For an efficient operation of the distribution systems, the DMSs must keep monitoring the real power loss consumed by the distribution lines. In other words, the DMSs should accurately estimate the total real power loss (P_{loss}) unless all the branches are monitored by the measuring units. In this context, the absolute error of P_{loss} can be a performance metric for the DSSE.

TABLE 6. Definition of the test cases.

Case	Meter type			
	Branch (POC)	Branch	Injection (load)	Injection (DG)
1	PMU-T5	SCADA	Smart meter	Smart meter
2	PMU-T5	PMU-T5	PMU-T5	PMU-T5
3	PMU-T5	SCADA	PMU-T5	PMU-T5
4	PMU-T5	SCADA	PMU-T4	PMU-T4
5	PMU-T5	SCADA	PMU-T3	PMU-T3
6	PMU-T5	SCADA	PMU-T2	PMU-T2
7	PMU-T5	SCADA	PMU-T1	PMU-T1
8	PMU-T5	SCADA	PMU-T0	PMU-T0
9	PMU-T5	PMU-T5	Smart meter	PMU-T5
10	PMU-T5	PMU-T5	PMU-T5	Smart meter
11	PMU-T5	PMU-T5	PMU-T4	PMU-T4
12	PMU-T5	SCADA	PMU-T5	Smart meter
13	PMU-T5	SCADA	PMU-T4	Smart meter
14	PMU-T5	SCADA	PMU-T3	Smart meter
15	PMU-T5	SCADA	PMU-T2	Smart meter
16	PMU-T5	SCADA	PMU-T1	Smart meter
17	PMU-T5	SCADA	PMU-T0	Smart meter

C. BASE AND BEST CASES

Table 6 shows that Case 1, which is a base case, has no PMU, except for the branch measurements at the POC, while all measurements in Case 2 are obtained by the T5-class PMUs. Table 7 presents the test results of these two cases indicating that all the T5-class PMU measurements drastically reduce the DSSE errors, including the TVEs of the voltage phasors, RMSEs, and power loss estimation errors. Additionally, the confidence level of Case 2 is 99.86%, which is much higher than that of Case 1.

Figs. 4 and 5 illustrate the TVEs of the voltage phasors at all buses and phases for Cases 1 and 2, respectively. The voltage TVEs in Case 1 slightly differ by buses, unlike in Case 2, because various meters with different accuracies are installed in Case 1.

Figs. 6 and 7 describe the absolute error of the P loss estimation at each branch for Cases 1 and 2, respectively, indicating that Case 2 yields a more accurate estimation of the P loss compared to Case 1. These figures illustrate that the absolute error of the P loss estimation at each branch depends on the meter accuracy near the branch. For example, in Case 1, the T5-class PMU at the POC considerably reduces

TABLE 7. Performance metrics of the case studies.

Case	Confidence level‡ (%)	TVE* of $\widetilde{V}$ (10^{-2}%)	RMSE† (10^{-6}pu)	$\lvert\mathcal{E}_{P_{loss}}\rvert$‡ (kW)
1	19.06	6.81	18.21	26.32
2	99.86	1.59	4.23	0.6804
3	98.12	1.96	5.21	1.131
4	1.64	3.10	8.31	1.16
5	0	13.83	37.2	1.91
6	0	54.98	146	6.14
7	0	1094	2700	45.9
8	0	9295	19900	440
9	47.82	2.11	5.65	6.423
10	44.36	1.78	4.73	0.927
11	2.04	2.28	6.13	0.687
12	58.38	2.38	6.40	14.23
13	2.08	3.62	9.80	14.29
14	0	15.67	42.7	14.95
15	0	61.93	166.5	19.59
16	0	1074	2756	84.15
17	0	9187	20052	5313

∗ The TVE is averaged over all the bus voltage phasors and samples.
‡ Each metric is averaged over all the samples.
† RMSE is averaged over all the states.

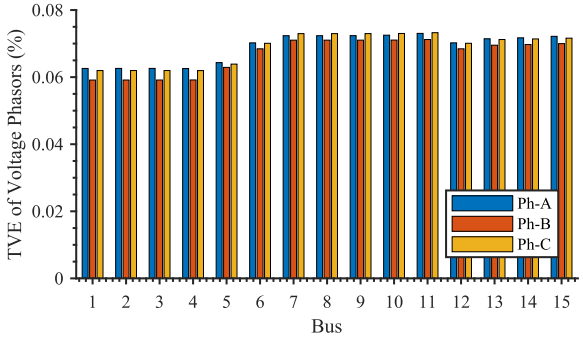

FIGURE 4. TVE of the voltage phasors at each bus in Case 1.

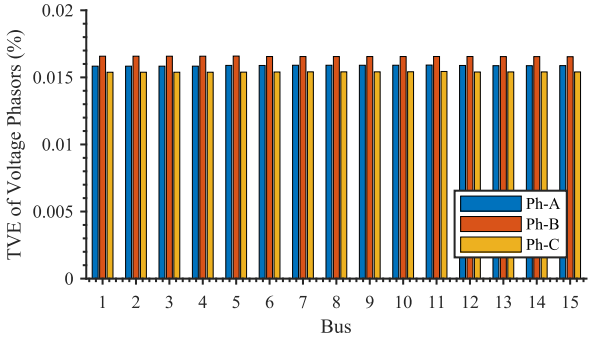

FIGURE 5. TVE of the voltage phasors at each bus in Case 2.

the absolute error of the P loss estimation at bus 1–2 and 2–3 branches compared with the other branches.

D. CONFIDENCE LEVEL CRITERION

Among all the test cases, the best case (i.e., Case 2) with all the T5-class PMUs installed shows the highest confidence

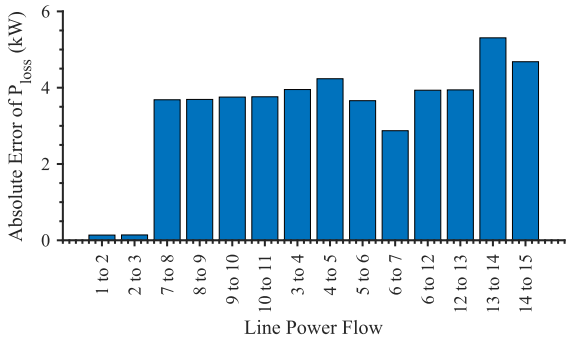

FIGURE 6. Absolute error of the *P* loss estimation at each branch in Case 1.

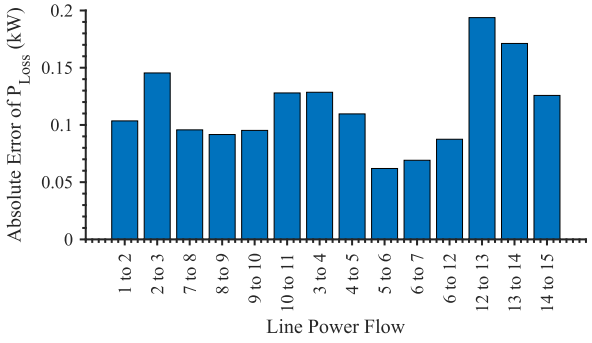

FIGURE 7. Absolute error of the *P* loss estimation at each branch in Case 2.

level of 99.86%. From this best case, the confidence level decreases to 98.12%, 47.82%, and 44.36% (refer to Table 7) when the T5-class PMUs are excluded and replaced by SCADA or smart meters at branches, load injections, and DG injections, respectively (i.e., Cases 3, 9, and 10, respectively). These results highlight that the T5-class PMUs must be installed at both the load and DG injections to obtain a confidence level of more than 95%, regardless of the type of branch measurements.

The results of Cases 4–8 show that the PMUs at the load and DG injections with an accuracy lower than that of the T5 class cannot improve the confidence level. In spite of the additional installation of the T5-class PMUs at the branches, it still needs to deploy the T5-class PMUs at both the load and DG injections to obtain high confidence levels (please refer to the results of Case 11 in Table 7).

The measurement redundancy in distribution systems is not enough to ensure high confidence levels [6]. Therefore, the accuracy of the PMUs is highly critical for obtaining estimation results with a high confidence level. The introduction of supplementary pseudo-measurements can improve the confidence level. Meanwhile, despite the low confidence levels, Cases 4 and 9–13 can still provide operating conditions with a relatively higher accuracy than the base case (i.e., Case 1), which can be observed from the TVEs, RMSEs, and $\lvert\mathcal{E}_{P_{loss}}\rvert$ metrics in Table 7.

E. TVE CRITERION OF THE VOLTAGE PHASORS

When the PMUs are installed only at the load injections, the minimum class that can meet the TVE requirement of 1%

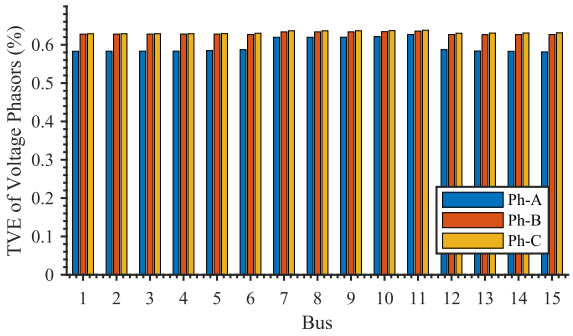

FIGURE 8. TVE of the voltage phasors at each bus in Case 15.

as regards the voltage phasors is T2 according to the simulation results of Cases 12–15 in Table 7. Fig. 8 shows the TVEs of the voltage phasors at all buses and phases for Case 15 with the T2-class PMUs, indicating that all of them are nearly 0.6%. However, at least a T4-class performance is required to obtain more accurate estimation results than the base case without the PMUs at the injections (refer to the results of Cases 2–4 and 9–13 in Table 7). Furthermore, a comparison of Cases 3–6 with Cases 12–15 depicts that the additional installation of the PMUs at the DG injections certainly reduces the TVE.

F. RMSE CRITERION

No specific requirement is provided for the RMSEs of the state variables, but one can observe a relative accuracy among various test cases using the RMSE metric. Table 7 presents the RMSE averaging in the states, noting that the RMSE considerably decreases with more PMUs installed or with the more accurate time-synchronization of the PMUs.

Similar to the TVE metrics, the test-cases with T4- or T5-class PMUs result in less RMSEs than the base case. The RMSE further significantly grows when the performance class of the PMUs becomes lower than T2 (i.e., T1 and T0). This trend is proven by the results of Cases 7, 8, 16, and 17 presented in Table 7.

G. CRITERION FOR $|\mathcal{E}_{P_{loss}}|$

Table 7 shows that the absolute error of the total line-loss estimation decreases when compared with the base case in most of the test cases, except for Cases 7, 8, 16, and 17, whose PMU performance is T0 or T1. The installation of the PMUs at both load and DG injections (i.e., Cases 3–8) also substantially improve the line-loss estimation in comparison with the PMU installations at only the load injections (i.e., Cases 12–17).

H. OBSERVATION ON THE IMPACT OF NON-GAUSSIAN PMU ERRORS

Thousands of field data have demonstrated that the PMU measurement error followed a non-Gaussian distribution with thick and long tails, such as the Student's t-distribution and the logistic distribution [42]. In this sense, we re-evaluate all the test-cases, with the PMU measurements whose errors obey the logistic distribution. Table 8 displays the test results, indicating that the three metrics (i.e., TVE, RMSE and $|\mathcal{E}_{P_{loss}}|$) are increased. These increases are natural because the PMU measurement errors follow the long- and thick-tailed distribution. Nevertheless, the observations on the TVE, RMSE, and $|\mathcal{E}_{P_{loss}}|$ are the same as those explained in Sections IV-E, -F, and -G. In other words, at least T4-class PMU installations at the load injections improve the TVE and RMSE metrics compared with the base case. Moreover, the installations of at least the T2-class PMU at both the load and DG injections considerably reduce the line-loss estimation error. Meanwhile, the confidence level degrades with the measurement errors under the logistic distribution compared with the Gaussian error cases. As aforementioned, a sufficient number of pseudo-measurements are required to improve the confidence level.

TABLE 8. Performance metrics of the case studies with the PMU measurement errors of the logistic distributions.

Case	Confidence level‡ (%)	TVE* of $\widetilde{V}$ (10^{-2}%)	RMSE† (10^{-6}pu)	$\lvert\mathcal{E}_{P_{loss}}\rvert$‡ (kW)
1	19.01	8.17	22.2	26.32
2	66.82	1.99	5.4	0.89
3	80.93	2.48	6.7	1.58
4	0	3.76	10.0	1.77
5	0	17.30	46.4	2.57
6	0	71.10	184.7	7.58
7	0	1509	3975	64.1
8	0	9263	19833	431
9	20.12	2.55	6.8	6.58
10	16.42	2.24	6.0	1.05
11	0	2.73	7.3	0.87
12	38.11	3.02	8.2	14.42
13	0	4.63	12.5	14.29
14	0	19.47	51.7	14.72
15	0	77.7	208.3	21.01
16	0	1470	3916	82.6
17	0	9177	20209	11153

∗ The TVE is averaged over all the bus voltage phasors and samples.
‡ Each metric is averaged over all the samples.
† RMSE is averaged over all the states.

I. OBSERVATION ON THE IMPACT OF PHASE IMBALANCE

Tables 3 and 5 show that the testbed is a three-phase system with phase imbalance, which is characterized by an asymmetric distribution line and an unbalanced load configuration. Hence, the testbed can represent the general distribution systems. This imbalance is reflected in Fig. 9, indicating that the RMSEs of the state variables certainly differ by buses and phases.

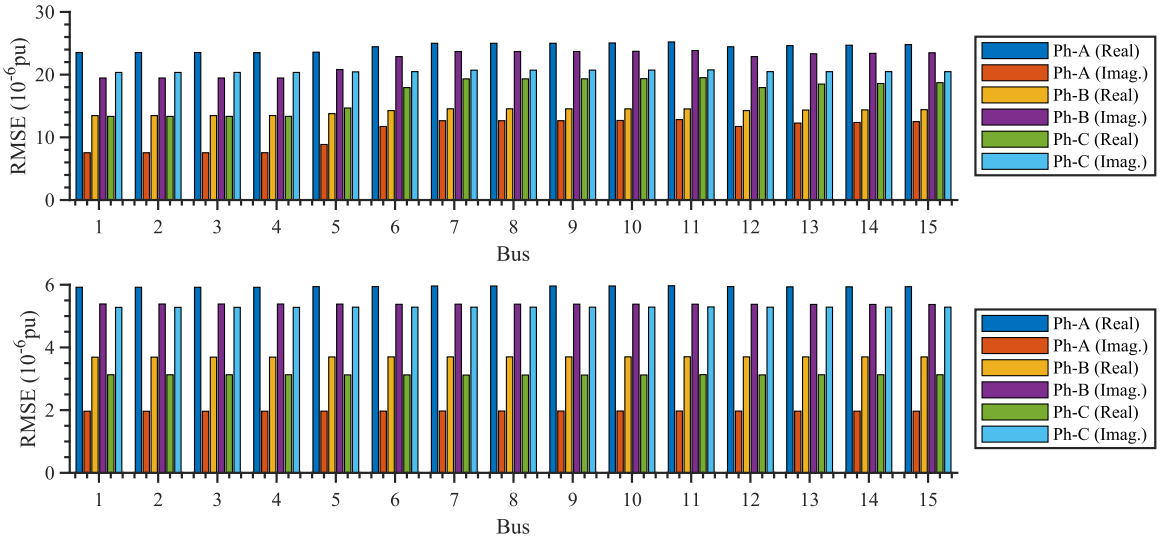

FIGURE 9. RMSE of the state variables at each bus in Case 1 (top) and 2 (bottom).

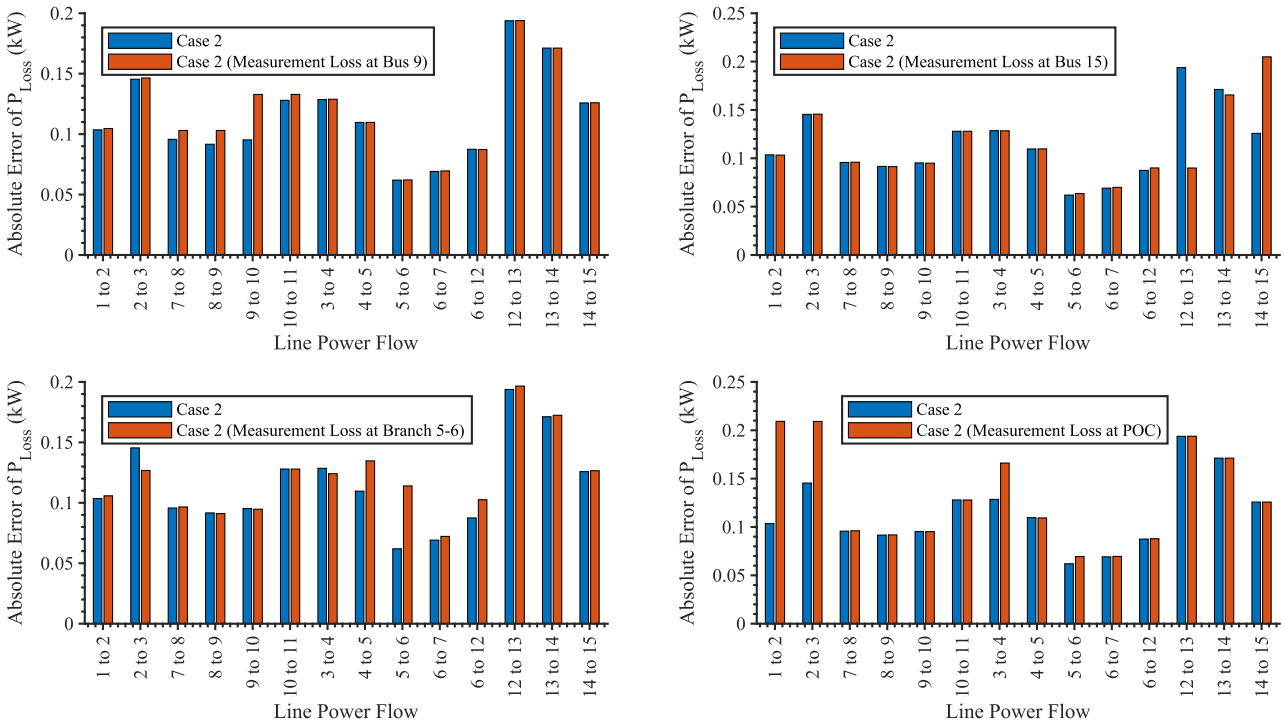

FIGURE 10. Comparison of the absolute errors of the line-loss estimation between Case 2 and the same case, except for the measurement loss at different locations.

J. OBSERVATION ON THE IMPACT OF MEASUREMENT LOSS

This section presents the results of the case studies on the missing measurement caused by communication delay or loss. The test cases are generated by subtracting from Case 2 the measurement at different locations: bus 9, bus 15, branch 5-to-6, and POC. Fig. 10 shows a comparison of Case 2 with the cases of the missing measurement in terms of the absolute error of the *P* loss estimation at each branch, pointing out that the missing measurement at a specific bus increases the error of the power flow through the bus and nearby buses (e.g., the measurement loss at the POC increases the absolute error of the *P* loss estimation at branches 1-to-2 and 2-to-3). Figs. 11 and 12 show the increased RMSEs of the state variables and the increased TVEs of the voltage phasors caused by the measurement loss at the POC, respectively. When comparing them with Figs. 5 and 9, the increased TVEs and RMSEs are negligible, but all the buses and phases are

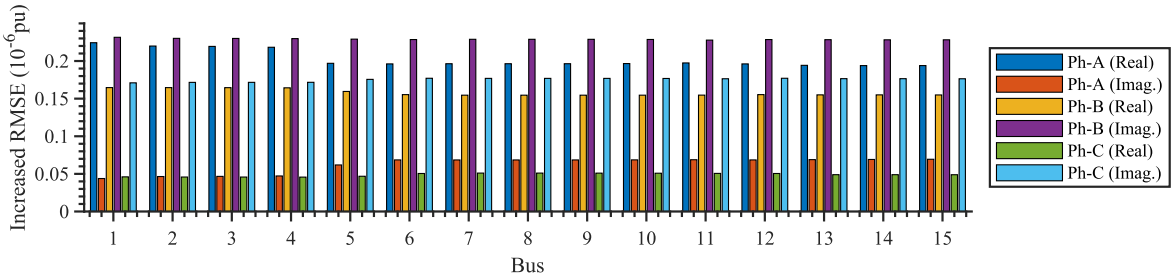

FIGURE 11. Increased RMSE of state variables caused by the measurement loss at POC in Case 2.

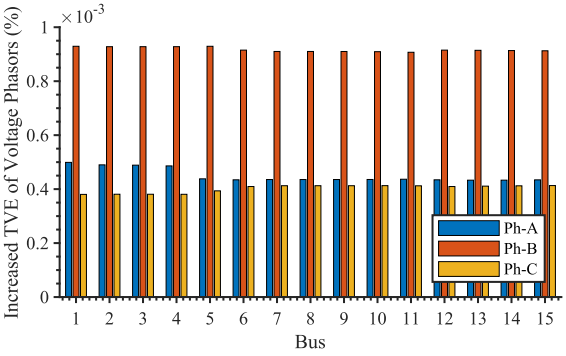

FIGURE 12. Increased TVE of the voltage phasors caused by the measurement loss at POC in Case 2.

affected by the missing measurement. All in all, the measurement loss affects the accuracy of the P loss estimation near the missing location but only slightly influences the TVEs of the voltage phasors and the RMSEs of the state variables.

V. DISCUSSIONS AND CONCLUSION

The application of the PMUs at the distribution systems can bring tremendous benefits to distribution system management in a way that overcomes the scarcity of measurements and improves the DSSE performance. However, a main obstacle to be tackled is the PMUs being relatively more expensive than smart meters due to GPS antennas and time-signal distributions. In this regard, this paper investigates the adequate and economic performance class of PMUs that can meet the proper performance of the DSSE by means of numerical experiments with a 15-bus test distribution system characterized by an unbalanced operation and an asymmetric structure.

The well-known WLS method is used for the DSSE implementation with a three-phase distribution line model and various measurement types, including voltage magnitude squared, real/reactive power, voltage/current phasor, and virtual measurements. This paper also defines the standard deviations of the PMU measurements based on uncertainty propagation theory to convert polar coordinates to Cartesian coordinates. Four performance metrics are defined to evaluate the DSSE results with respect to accuracy: confidence level, TVE, RMSE, and absolute error of the total line-loss estimation.

Various test cases are set up according to the meter types (i.e., PMUs, SCADA systems, and smart meters) at the specific locations of the test systems, such as the POC, branches, and load/DG injections. The criteria for the PMU performance classes that can meet the proper DSSE performance are investigated after numerical simulations. Note that the observability of the test system is guaranteed in all the case studies because the system has a sufficient number of independent measurements, which is larger than the number of the state variables.

First, the high confidence level can be achieved by deploying T5-class PMUs, which is the most accurate among all the classes, at both load and DG injections; otherwise, the confidence level significantly declines mainly because of the lack of redundancy in the measurements. However, if at least T4-class PMUs are installed at the load injections, the TVEs of the voltage phasors and the RMSEs reduce compared to those in the base case without PMUs at the injections. Finally, the absolute error of the total line-loss estimation can decrease with the PMU installation, of which the classes are above T1 at the load injections. The error can be further reduced by additional deployment at the DG injections.

This paper further evaluates the criteria under realistic conditions such as cases with non-Gaussian PMU errors, phase imbalance, and measurement loss. The PMU measurements with the non-Gaussian errors that follow the long- and thick-tailed distribution degrade the confidence level but have little influence on the other three metrics. The phase imbalance has a moderate impact on the RMSE of the states, and the measurement loss deteriorates the accuracy of the absolute errors of the line-loss estimation.

Table 9 compares the performance metrics in various perspectives based on the test results. Among them, the TVE of the voltage phasor is the most reliable, despite the non-Gaussian PMU errors, phase imbalance, and measurement loss. The confidence level is useful for obtaining the estimation results with a high accuracy because of its high sensitivity to the measurement errors. The RMSE and the absolute error of the line-loss estimation can also be phase imbalance indicators. Moreover, the absolute error of the total line-loss estimation requires the minimum accuracy of the T2-class to improve the performance from the base case, which has no PMU. In the end, the distribution system

TABLE 9. Comparison of the performance criteria.

Metric	Requirements for the performance improvement from base case	Impact of non-Gaussian PMU errors	Impact of phase imbalance	Impact of measurement loss
Confidence level	PMU-T5 at load and DG injections	Huge	Little	Little
TVE of $\widetilde{V}$	Minimum PMU-T4 at load injections	Little	Little	Little
RMSE	Minimum PMU-T4 at load injections	Little	Moderate	Little
$\lvert\mathcal{E}_{P_{loss}}\rvert$	Minimum PMU-T2 at load injections	Little	Moderate	Huge

operator must select proper performance criteria in light of operational applications that use the DSSE results.

Note that the PMU performance criteria might vary in the structure and parameters of distribution systems. The key contribution of this paper is the methodology used to find the adequate PMU accuracy and their installation sites that can improve the DSSE performance and overall accuracy. In the end, the PMU accuracy at specific sites can be selected in accordance with the present PMU standards.

REFERENCES

[1] T. Wu, C. Y. Chung, and I. Kamwa, "A fast state estimator for systems including limited number of PMUs," *IEEE Trans. Power Syst.*, vol. 32, no. 6, pp. 4329–4339, Nov. 2017.

[2] L. Zhang, A. Bose, A. Jampala, V. Madani, and J. Giri, "Design, testing, and implementation of a linear state estimator in a real power system," *IEEE Trans. Smart Grid*, vol. 8, no. 4, pp. 1782–1789, Jul. 2017.

[3] E. Ghahremani and I. Kamwa, "Dynamic state estimation in power system by applying the extended Kalman filter with unknown inputs to phasor measurements," *IEEE Trans. Power Syst.*, vol. 26, no. 4, pp. 2556–2566, Nov. 2011.

[4] M. Jamei, A. Scaglione, C. Roberts, E. Stewart, S. Peisert, C. McParland, and A. McEachern, "Anomaly detection using optimally placed μPMU sensors in distribution grids," *IEEE Trans. Power Syst.*, vol. 33, no. 4, pp. 3611–3623, Jul. 2018.

[5] W. Jiang, V. Vittal, and G. T. Heydt, "A distributed state estimator utilizing synchronized phasor measurements," *IEEE Trans. Power Syst.*, vol. 22, no. 2, pp. 563–571, May 2007.

[6] A. Primadianto and C.-N. Lu, "A review on distribution system state estimation," *IEEE Trans. Power Syst.*, vol. 32, no. 5, pp. 3875–3883, Sep. 2017.

[7] K. Dehghanpour, Z. Wang, J. Wang, Y. Yuan, and F. Bu, "A survey on state estimation techniques and challenges in smart distribution systems," *IEEE Trans. Smart Grid*, vol. 10, no. 2, pp. 2312–2322, Mar. 2019.

[8] S. Lefebvre, J. Prévost, and L. Lenoir, "Distribution state estimation: A necessary requirement for the smart grid," in *Proc. IEEE PES Gen. Meeting Conf. Expo.*, Jul. 2014, pp. 1–5.

[9] I. Džafić and R. A. Jabr, "Real time multiphase state estimation in weakly meshed distribution networks with distributed generation," *IEEE Trans. Power Syst.*, vol. 32, no. 6, pp. 4560–4569, Nov. 2017.

[10] X. Yang, Z. Wei, G. Sun, Y. Yuan, Y. Sun, and H. Shen, "Distribution system state estimation considering the characteristics of power electronic loads," in *Proc. IEEE Power Energy Soc. Gen. Meeting*, Jul. 2014, pp. 1–5.

[11] W. Gu, G. Lou, W. Tan, and X. Yuan, "A nonlinear state estimator-based decentralized secondary voltage control scheme for autonomous microgrids," *IEEE Trans. Power Syst.*, vol. 32, no. 6, pp. 4794–4804, Nov. 2017.

[12] S. Deshmukh, B. Natarajan, and A. Pahwa, "State estimation and voltage/VAR control in distribution network with intermittent measurements," *IEEE Trans. Smart Grid*, vol. 5, no. 1, pp. 200–209, Jan. 2014.

[13] M. Pau, F. Ponci, A. Monti, S. Sulis, C. Muscas, and P. A. Pegoraro, "An efficient and accurate solution for distribution system state estimation with multiarea architecture," *IEEE Trans. Instrum. Meas.*, vol. 66, no. 5, pp. 910–919, May 2017.

[14] X. Kong, Z. Yan, R. Guo, X. Xu, and C. Fang, "Three-stage distributed state estimation for AC-DC hybrid distribution network under mixed measurement environment," *IEEE Access*, vol. 6, pp. 39027–39036, 2018.

[15] S. Choi and A. P. S. Meliopoulos, "Effective real-time operation and protection scheme of microgrids using distributed dynamic state estimation," *IEEE Trans. Power Del.*, vol. 32, no. 1, pp. 504–514, Feb. 2017.

[16] H. Mohsenian-Rad, E. Stewart, and E. Cortez, "Distribution synchrophasors: Pairing big data with analytics to create actionable information," *IEEE Power Energy Mag.*, vol. 16, no. 3, pp. 26–34, May 2018.

[17] C. Carquex, C. Rosenberg, and K. Bhattacharya, "State estimation in power distribution systems based on ensemble Kalman filtering," *IEEE Trans. Power Syst.*, vol. 33, no. 6, pp. 6600–6610, Nov. 2018.

[18] C. Muscas, M. Pau, P. A. Pegoraro, and S. Sulis, "Uncertainty of voltage profile in PMU-based distribution system state estimation," *IEEE Trans. Instrum. Meas.*, vol. 65, no. 5, pp. 988–998, May 2016.

[19] M. G. Damavandi, V. Krishnamurthy, and J. R. Marti, "Robust meter placement for state estimation in active distribution systems," *IEEE Trans. Smart Grid*, vol. 6, no. 4, pp. 1972–1982, Jul. 2015.

[20] *IRIG Serial Time Code Formats*, Standard 200-16, IRIG, White Sands Missile Range, NM, USA, Aug. 2016, pp. 1–64.

[21] *Network Time Protocol Version 4: Protocol and Algorithms Specification*, document RFC 5905, Jun. 2010, pp. 1–110.

[22] *IEEE Standard for a Precision Clock Synchronization Protocol for Networked Measurement and Control Systems*, IEEE Standard 1588-2008, New York, NY, USA, Jul. 2008, pp. 1–300.

[23] *IEEE Standard Profile for Use of IEEE 1588 Precision Time Protocol in Power System Applications*, IEEE Standard C37.238-2017, New York, NY, USA, Jun. 2017, pp. 1–42.

[24] *IEEE Standard for Synchrophasor Data Transfer for Power Systems*, IEEE Standard C37.118.2-2011, New York, NY, USA, Dec. 2011, pp. 1–53.

[25] *IEEE Guide for Synchronization, Calibration, Testing, and Installation of Phasor Measurement Units (PMUs) for Power System Protection and Control*, IEEE Standard C37.242-2013, New York, NY, Mar. 2013, pp. 1–107.

[26] A. J. Roscoe, I. F. Abdulhadi, and G. M. Burt, "P and M class phasor measurement unit algorithms using adaptive cascaded filters," *IEEE Trans. Power Del.*, vol. 28, no. 3, pp. 1447–1459, Jul. 2013.

[27] A. J. Roscoe, "Exploring the relative performance of frequency-tracking and fixed-filter phasor measurement unit algorithms under C37.118 test procedures, the effects of interharmonics, and initial attempts at merging P-class response with M-class filtering," *IEEE Trans. Instrum. Meas.*, vol. 62, no. 8, pp. 2140–2153, Aug. 2013.

[28] P. Castello, J. Liu, A. Monti, C. Muscas, P. A. Pegoraro, and F. Ponci, "Toward a class 'P+M' phasor measurement unit," in *Proc. IEEE Int. Workshop Appl. Meas. Power Syst. (AMPS)*, Sep. 2013, pp. 91–96.

[29] A. von Meier, E. Stewart, A. McEachern, M. Andersen, and L. Mehrmanesh, "Precision micro-synchrophasors for distribution systems: A summary of applications," *IEEE Trans. Smart Grid*, vol. 8, no. 6, pp. 2926–2936, Nov. 2017.

[30] J. H. Eto, E. Stewart, T. Smith, M. Buckner, H. Kirkham, F. Tuffner, and D. Schoenwald, "Scoping study on research and development priorities for distribution-system phasor measurement units," Ernest Orlando Lawrence Berkeley Nat. Lab., Berkeley, CA, USA, Tech. Rep. SAND2016-3546R, Apr. 2016.

[31] *Communication Networks and Systems for Power Utility Automation—Part 5: Communication Requirements for Functions and Device Models*, Standard IEC 61850-5:2013, Ed. 2.0, Jan. 2013, pp. 1–306.

[32] A. P. Meliopoulos. Synchrophasor Measurement Accuracy Characterization. North American Synchrophasor Initiative Performance & Standards Task Team, Aug. 2007. [Online]. Available: https://www.naspi.org
[33] A. P. S. Meliopoulos, G. J. Cokkinides, C. Hedrington, and T. L. Conrad, "The supercalibrator—A fully distributed state estimator," in *Proc. IEEE Power Energy Soc. Gen. Meeting*, Jul. 2010, pp. 1–8.
[34] J. Du, S. Ma, Y.-C. Wu, and H. V. Poor, "Distributed hybrid power state estimation under pmu sampling phase errors," *IEEE Trans. Signal Process.*, vol. 62, no. 16, pp. 4052–4063, Aug. 2014.
[35] R. Singh, B. C. Pal, and R. A. Jabr, "Choice of estimator for distribution system state estimation," *IET Gener., Transmiss. Distrib.*, vol. 3, no. 7, pp. 666–678, Jul. 2009.
[36] A. Shahsavari, A. Sadeghi-Mobarakeh, E. M. Stewart, E. Cortez, L. Alvarez, F. Megala, and H. Mohsenian-Rad, "Distribution grid reliability versus regulation market efficiency: An analysis based on micro-PMU data," *IEEE Trans. Smart Grid*, vol. 8, no. 6, pp. 2916–2925, Nov. 2017.
[37] X. Wang, X. Xie, S. Zhang, L. Luo, Y. Liu, G. Sheng, and X. Jiang, "Micro-PMU for distribution power lines," *CIRED-Open Access Proc. J.*, vol. 2017, no. 1, pp. 333–337, 2017.
[38] A. Abur and A. G. Expósito, *Power System State Estimation: Theory and Implementation*. New York, NY, USA: Marcel Dekker, 2004.
[39] S. Chakrabarti and E. Kyriakides, "PMU measurement uncertainty considerations in WLS state estimation," *IEEE Trans. Power Syst.*, vol. 24, no. 2, pp. 1062–1071, May 2009.
[40] S. Choi, "Practical coordination between day-ahead and real-time optimization for economic and stable operation of distribution systems," *IEEE Trans. Power Syst.*, vol. 33, no. 4, pp. 4475–4487, Jul. 2018.
[41] W. H. Kersting, "Radial distribution test feeders," *IEEE Trans. Power Syst.*, vol. 6, no. 3, pp. 975–985, Aug. 1991.
[42] S. Wang, J. Zhao, Z. Huang, and R. Diao, "Assessing Gaussian assumption of PMU measurement error using field data," *IEEE Trans. Power Del.*, vol. 33, no. 6, pp. 3233–3236, Dec. 2018.

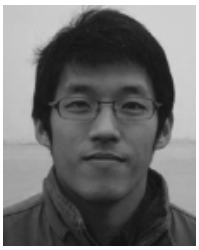

JONGHOEK KIM (M'18) received the B.S. degree in electrical and computer engineering from Yonsei University, South Korea, in 2006, the M.S. degree in electrical and computer engineering from the Georgia Institute of Technology, USA, in 2008, and the Ph.D. degree from the Georgia Institute of Technology, in 2011, co-advised by Dr. F. Zhang and Dr. M. Egerstedt. He was a Senior Researcher with the Agency for Defense Development, South Korea, from 2011 to 2018. He is currently an Assistant Professor with Hongik University, South Korea. His research interests include target tracking, control theory, robotics, multi-agent systems, and optimal estimation.

HYUN-TAE KIM received the B.E. degree in electronic engineering from Gachon University, South Korea, in 2016. He is currently pursuing the M.S. degree in electrical engineering with Korea University, Seoul, South Korea. He was a Researcher with Hyundai Power System, South Korea, from 2015 to 2017. His research interest includes microgrid operation and planning.

SUNGYUN CHOI (M'14) received the B.E. degree in electrical engineering from Korea University, Seoul, South Korea, in 2002, and the M.S. and Ph.D. degrees in electrical and computer engineering from the Georgia Institute of Technology, Atlanta, GA, USA, in 2009 and 2013, respectively. From 2002 to 2005, he was a Network and System Engineer, and from 2014 to 2018, he was a Senior Researcher with the Smart Power Grid Research Center, Korea Electrotechnology Research Institute, Uiwang, South Korea. Since 2018, he has been an Assistant Professor with the School of Electrical Engineering, Korea University. His research interests include smart grid technology, microgrid operation, control, and protection, power system state estimation, phasor measurement units, and sub-synchronous oscillations.